

## Electronic Supplemental Information

### Coexisting Order and Disorder Within a Common 40-Residue Amyloid- $\beta$ Fibril Structure in Alzheimer's Disease Brain Tissue

Ujjayini Ghosh, Wai-Ming Yau, and Robert Tycko

Laboratory of Chemical Physics, National Institute of Diabetes and Digestive and Kidney Diseases

National Institutes of Health, Bethesda, Maryland 20892-0520, U.S.A.

#### Materials and Methods

##### *Fibril preparation*

Specifically labeled A $\beta$ 40 peptides were synthesized with a Protein Technologies Tribute synthesizer using Fmoc solid phase peptide synthesis (amino acid sequence NH<sub>2</sub>-DAEFRHDSGYEVHHQKLVFF AEDVGSNKGAIIGLMVGGVV-COOH) and an Fmoc-Val Wang resin (0.4 meq/g). Purification was done by reverse-phase HPLC with acetonitrile/water gradient using a preparative C18 column and resulted in >95% purity, as estimated from liquid chromatography-mass spectrometry with electrospray ionization.

To prepare second-generation fibrils, the first-generation PCA3f sample of Qiang *et al.*<sup>3</sup> was unpacked from its magic-angle spinning (MAS) rotor, then resuspended in fibril growth buffer (10 mM phosphate buffer, pH 7.4, with 0.01% w/v sodium azide) and sonicated to break the PCA3f fibrils into fragments. A 10% portion of this material was used as seeds for second-generation fibrils. After dilution of the seeds in fibril growth buffer to a total volume of 2.4 ml, 1.0 mg of specifically labeled A $\beta$ 40 was dissolved in 50  $\mu$ l of dimethyl sulfoxide and added to the seed solution. Fibril growth then proceeded by incubation at room temperature without stirring or agitation of the solution. Each fibril solution was self-seeded 1-2 days after initial seeding. Self-seeding was done by taking an aliquot (~5% by volume) from the fibril solution, sonicating it briefly, and returning it to the same fibril solution. Self-seeded solutions were then incubated for an additional 5-6 days before pelleting and lyophilization for ssNMR. TEM images were recorded after the first overnight incubation, and also before pelleting.

Third-generation fibrils were prepared in the same way, but using approximately 5% by mass of second-generation fibrils as the seeds.

Fibrils were pelleted by ultracentrifugation for 2 h at 176,000 x g and 4° C. The supernatant was discarded and the pellet was resuspended in 3-5  $\mu$ l of deionized water, then lyophilized. Lyophilized fibrils were packed into 1.8 mm MAS rotors, rehydrated with 5-10  $\mu$ l of fibril growth buffer, then centrifuged at 17,000 x g at 20 °C for 5-35 min. Excess buffer was removed before capping the MAS rotor.

##### *Electron microscopy*

Negatively-stained TEM images were obtained with an FEI Morgagni microscope, operating at 80 kV and equipped with an AMT Advantage HR CCD camera. Samples were diluted

ten times in deionized water. A 10  $\mu$ l aliquot of the diluted sample was then adsorbed onto a glow-discharged carbon film on a lacey-carbon-coated copper mesh grid. The grid was blotted, washed with 10  $\mu$ l of deionized water, blotted, stained with 2% uranyl acetate solution, blotted, and dried in air.

### *ssNMR spectroscopy*

2D and 3D ssNMR spectra were acquired at 14.1 T (599.1 MHz  $^1\text{H}$  NMR frequency), using a Varian InfinityPlus spectrometer and a 1.8 mm MAS probe produced by the laboratory of Dr. Ago Samoson (Tallinn University of Technology, Estonia). Sample temperatures were approximately 25° C. An MAS frequency of 13.6 kHz,  $^1\text{H}$  decoupling fields of 100 kHz, and 1.0 s recycle delays were used for all spectra.

2D  $^{13}\text{C}$ - $^{13}\text{C}$  ssNMR spectra were acquired with 50 ms DARR mixing periods.<sup>4</sup>  $^1\text{H}$ - $^{13}\text{C}$  cross-polarization contact times were 1.5 ms, with 63 kHz  $^1\text{H}$  fields and ramped  $^{13}\text{C}$  fields centered at approximately 50 kHz. Data sets contained 186 complex  $t_1$  points and 512 complex  $t_2$  points, with 46.3 kHz and 66.7 kHz spectral widths in  $t_1$  and  $t_2$  dimensions, respectively. 2D  $^{15}\text{N}$ - $^{13}\text{C}$  spectra were acquired with 4.0 ms band-selective  $^{15}\text{N}$ - $^{13}\text{C}$  cross-polarization between  $t_1$  and  $t_2$ , with 9.0 kHz  $^{15}\text{N}$  fields and approximately 23 kHz  $^{13}\text{C}$  fields.  $^1\text{H}$ - $^{15}\text{N}$  cross-polarization used 52 kHz  $^1\text{H}$  fields and ramped  $^{15}\text{N}$  fields centered at approximately 38 kHz. Data sets contained 80 complex  $t_1$  points and 512 complex  $t_2$  points, with 9.0 kHz and 66.7 kHz spectral widths in  $t_1$  and  $t_2$  dimensions, respectively. 2D spectra were processed with 50-80 Hz Gaussian line broadening in both dimensions. Total data acquisition times were 24-48 h for 2D  $^{13}\text{C}$ - $^{13}\text{C}$  spectra and 48-36 h for 2D  $^{15}\text{N}$ - $^{13}\text{C}$  spectra.

The 3D NCACX spectrum of uniformly  $^{15}\text{N}$ ,  $^{13}\text{C}$ -labeled A $\beta$ 40 fibrils was acquired with a DARR mixing time of 50 ms, and with 36 and 32 complex points and 4.72 kHz and 4.72 kHz spectral widths in the  $t_1$  and  $t_2$  dimensions, respectively. A total of 120 scans were acquired for each free-induction decay. Other conditions were the same as in 2D  $^{15}\text{N}$ - $^{13}\text{C}$  spectra. The 3D NCOX spectrum was acquired with the same conditions, but with a total of 80 scans for each free-induction decay.

Spectra were referenced externally to the  $^{13}\text{CO}$  signal of L-alanine powder at 179.65 ppm (relative to DSS). Data were processed and displayed with NMRPipe (available from <https://www.ibbr.umd.edu/nmrpipe/>) and Sparky (available from <https://www.cgl.ucsf.edu/home/sparky/>) software.

### **ESI references**

1. A. K. Paravastu, R. D. Leapman, W. M. Yau and R. Tycko, *Proc. Natl. Acad. Sci. U. S. A.*, 2008, **105**, 18349-18354.
2. Y. Ishii, *J. Chem. Phys.*, 2001, **114**, 8473-8483.
3. W. Qiang, W. M. Yau, J. X. Lu, J. Collinge and R. Tycko, *Nature*, 2017, **541**, 217-221.
4. K. Takegoshi, S. Nakamura and T. Terao, *J. Chem. Phys.*, 2003, **118**, 2325-2341.
5. Y. Shen and A. Bax, *J. Biomol. NMR*, 2013, **56**, 227-241.
6. J. X. Lu, W. Qiang, W. M. Yau, C.D. Schwieters, S. C. Meredith, and R. Tycko, *Cell*, 2013, **154**, 1257-1268.

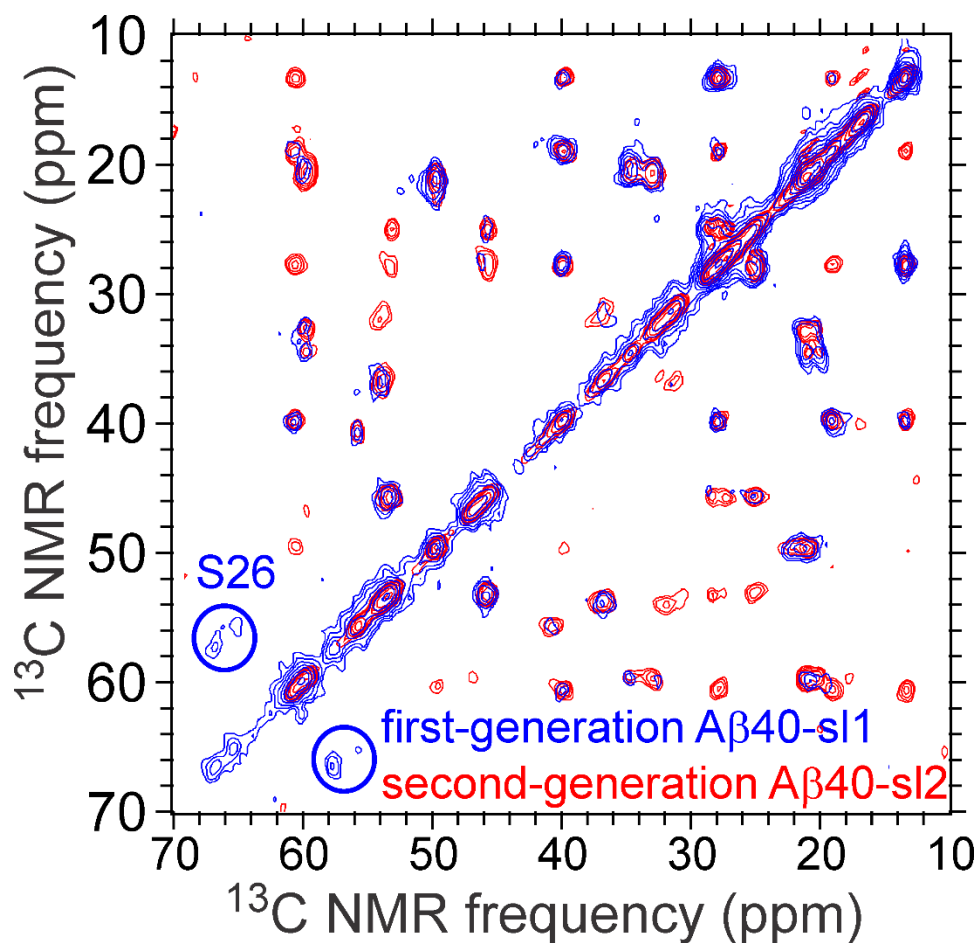


Figure S1: Superposition of 2D  $^{13}\text{C}$ - $^{13}\text{C}$  NMR spectra of first-generation A $\beta$ 40-s11 (blue) and second-generation A $\beta$ -s12 (red) fibrils. Positions of one-bond crosspeaks are in good agreement, indicating accurate propagation of the molecular structure from the first-generation to the second-generation. Mixing periods were 2.35 ms fpRFDR<sup>2</sup> for the A $\beta$ 40-s11 spectrum and 50 ms DARR<sup>4</sup> for the A $\beta$ 40-s12 spectrum, accounting for differences in multiple-bond crosspeaks amplitudes. S26 was isotopically labeled in A $\beta$ 40-s11, but not in A $\beta$ 40-s12.

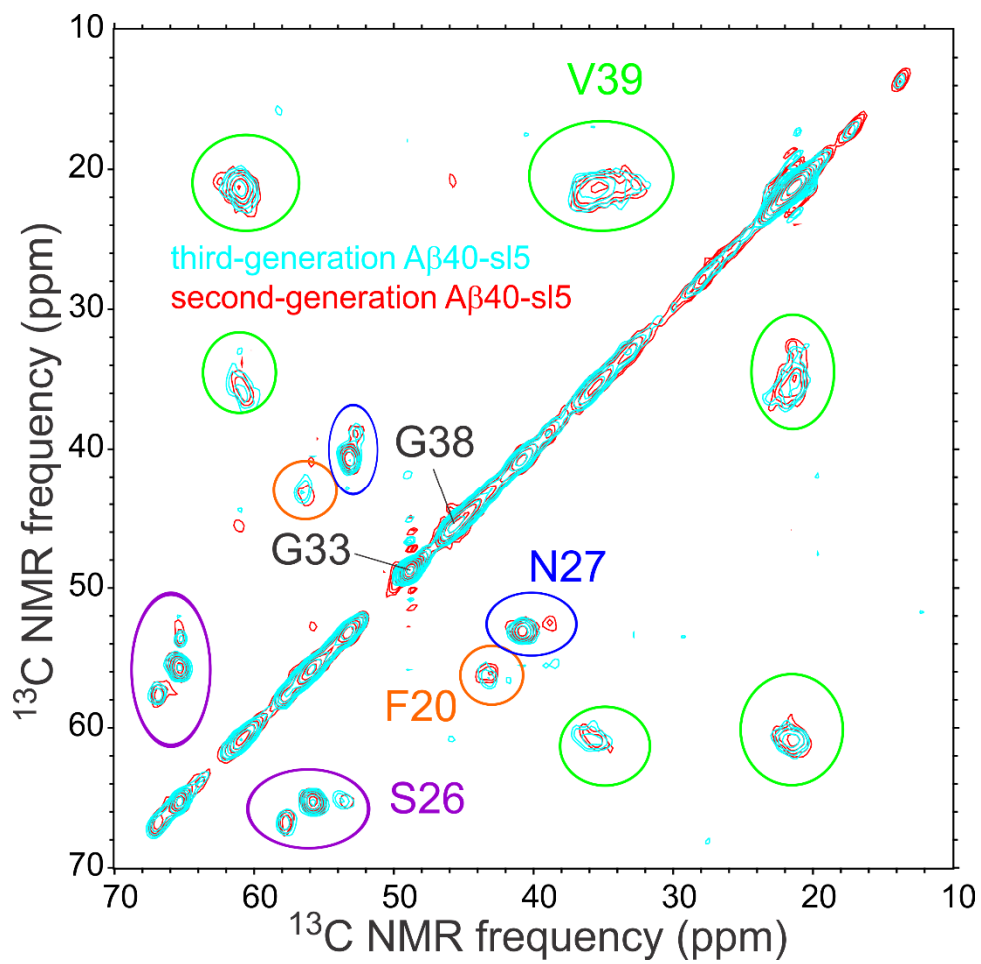


Figure S2: Superposition of 2D  $^{13}\text{C}$ - $^{13}\text{C}$  NMR spectra of second-generation (red) and third-generation (cyan) A $\beta$ 40-s15 fibrils. The good agreement of crosspeak positions indicates accurate propagation of the molecular structure from the second generation to the third generation.

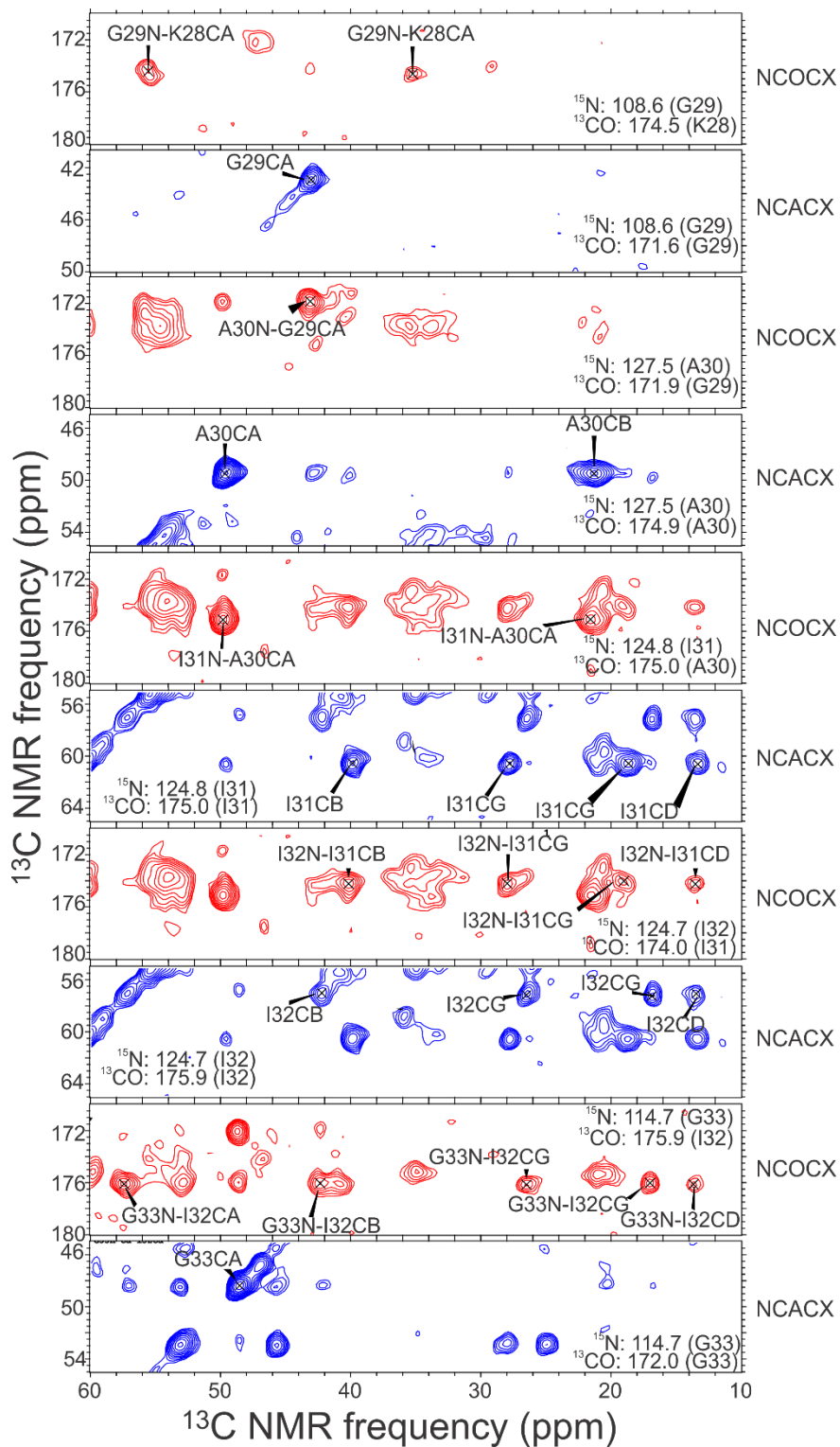


Figure S3: Representative strip plots from 3D NCOCX (red) and NCACX (blue) spectra of uniformly  $^{15}\text{N}$ ,  $^{13}\text{C}$ -labeled  $\text{A}\beta_{40}$  fibrils, showing chemical shift assignments for residues 29-33. 2D planes are taken at  $^{15}\text{N}$  NMR frequencies indicated in each plot. Contour levels of the increase by successive factors of 1.4.

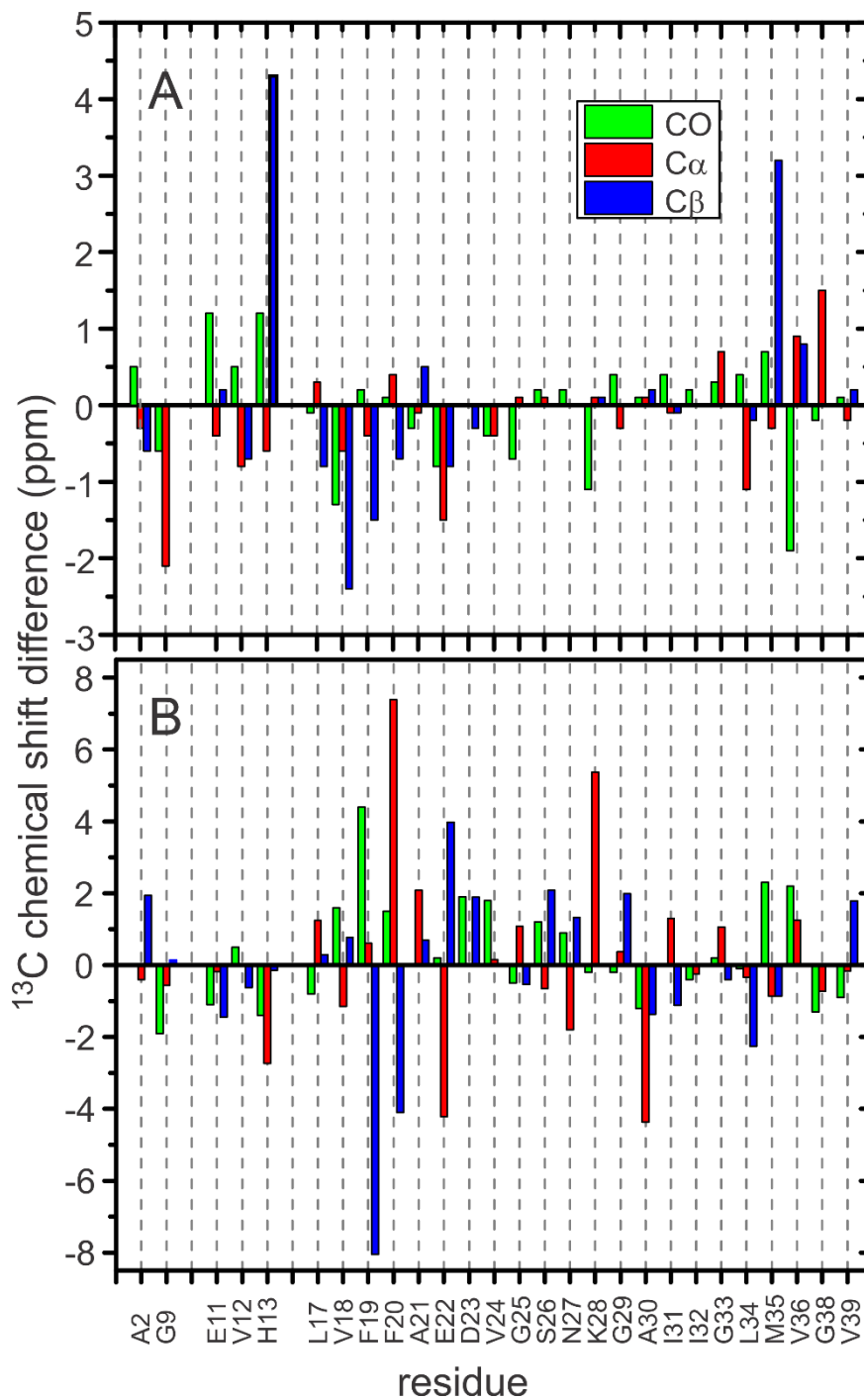


Figure S4: (A) Site-specific differences in  $^{13}\text{C}$  chemical shifts between A $\beta$ 40 fibrils prepared *in vitro* by Paravastu *et al.*<sup>1</sup> (BioMagResBank code 18129) and brain-derived A $\beta$ 40 fibrils discussed in this paper. Although these two types of fibrils have similar morphologies in TEM images, the chemical shift differences indicate differences in molecular structure. (B) Site-specific differences in  $^{13}\text{C}$  chemical shifts between brain-derived A $\beta$ 40 fibrils from patient 1 of Lu *et al.*<sup>6</sup> (BioMagResBank code 19009) and brain-derived A $\beta$ 40 fibrils discussed in this paper.

Table S1:  $^{15}\text{N}$  and  $^{13}\text{C}$  chemical shifts in brain-derived A $\beta$ 40 fibrils, in parts-per-million relative to liquid  $\text{NH}_3$  and 4,4-dimethyl-4-silapentane-1-sulfonic acid, respectively. Uncertainties are full widths of crosspeaks at half height. Predicted  $\phi, \psi$  torsion angles are from the TALOS-N program.<sup>5</sup>

Residue	CO	C $\alpha$	C $\beta$	C $\gamma$	C $\delta$	C $\epsilon$	N	Predicted $\phi, \psi$ values (degrees)
A2	175.2 $\pm 0.7$	50.5 $\pm 0.8$	22.2 $\pm 0.9$				120.6 $\pm 1.5$	
D7	175.5 $\pm 1.8$	52.5 $\pm 1.1$	42.2	179.6 $\pm 0.9$			127.5 $\pm 1.0$	
G9	171.6 $\pm 0.9$	44.1 $\pm 0.8$					-	
E11	174.4 $\pm 0.9$	54.1 $\pm 1.0$	33.6		182.7 $\pm 0.8$		126.4 $\pm 1.5$	-104.2 $\pm$ 12.9, 132.1 $\pm$ 12.1
V12	174.6 $\pm 1.1$	60.2 $\pm 0.8$	34.7 $\pm 1.4$	20.6 $\pm 1.1$			124.2 $\pm 1.4$	-114.3 $\pm$ 8.9, 130.9 $\pm$ 6.4
H13	174.1	53.6 $\pm 1.0$	31.7	134.3			120.0	-132.6 $\pm$ 12.5, 147.6 $\pm$ 10.1
L17	174.6 $\pm 0.9$	54.2 $\pm 0.8$	44.1 $\pm 1.0$	-	-		126.8 $\pm 0.9$	-110.1 $\pm$ 10.9, 125.6 $\pm$ 10.6
V18	172.8 $\pm 0.7$	60.0 $\pm 0.6$	32.9 $\pm 0.6$	20.4 $\pm 0.6$			120.9 $\pm$ 1.2	-106.9 $\pm$ 11.6, 129.1 $\pm$ 8.5
F19	172.9 $\pm 0.7$	55.7 $\pm 0.5$	40.7 $\pm 0.6$	132.3	138.2	131.0	125.7 $\pm 0.8$	-108.7 $\pm$ 9.6, 127.5 $\pm$ 8.3
F20	172.4 $\pm 0.7$	56.4 $\pm 0.6$	42.2				126.7 $\pm 1.3$	-116.9 $\pm$ 9.8, 127.3 $\pm$ 8.0
A21	174.8 $\pm 0.7$	49.6 $\pm 0.8$	22.6 $\pm 0.8$				128.7 $\pm 1.5$	-124.3 $\pm$ 15.3, 137.3 $\pm$ 15.8
E22	175.2 $\pm 0.8$	52.9 $\pm 0.6$	33.1 $\pm 0.7$	34.6 $\pm 0.6$	180.3 $\pm 0.5$		120.1 $\pm 1.2$	-128.6 $\pm$ 11.6, 139.7 $\pm$ 11.6
D23	174.4 $\pm 0.6$	56.5 $\pm 0.6$	38.8 $\pm 0.5$	183.0 $\pm 0.5$			122.7 $\pm 1.2$	-126.6 $\pm$ 21.9, 141.2 $\pm$ 16.3
V24	176.4 $\pm 0.9$	59.7 $\pm 0.8$	32.7 $\pm 0.8$	20.7 $\pm 1.0$			121.7 $\pm 1.2$	-122.0 $\pm$ 19.2, 132.5 $\pm$ 12.5
G25	170.8 $\pm 1.0$	46.6 $\pm 0.8$					115.5 $\pm 1.1$	-139.3 $\pm$ 26.4, 162.3 $\pm$ 23.4
S26	174.0 $\pm 0.6$	55.8 $\pm 0.6$	65.3 $\pm 0.5$				107.5 $\pm 0.9$	-144.3 $\pm$ 12.7, 154.9 $\pm$ 10.5
N27	174.5 $\pm 1.0$	53.1 $\pm 0.7$	40.8 $\pm 0.9$	176.4 $\pm 0.8$			115.2 $\pm 1.1$	
K28	174.2 $\pm 0.9$	55.6 $\pm 0.8$	35.6 $\pm 1.0$	29.9 $\pm 1.2$	27.9 $\pm 1.0$	42.8 $\pm 1.0$	126.8 $\pm 1.0$	-129.6 $\pm$ 15.2, 148.4 $\pm$ 15.4
G29	172.1 $\pm 0.6$	43.2 $\pm 1.1$					108.7 $\pm 1.5$	
A30	175.3 $\pm 0.6$	49.9 $\pm 0.7$	21.5 $\pm 1.2$				127.6 $\pm 1.0$	-114.9 $\pm$ 10.4, 128.1 $\pm$ 10.1
I31	174.0 $\pm 0.6$	60.7 $\pm 0.7$	39.8 $\pm 0.4$	27.8 $\pm$ 0.4, 19.0 $\pm$ 0.4	13.3 $\pm 0.5$		124.8 $\pm 1.1$	-107.6 $\pm$ 11.3, 125.1 $\pm$ 7.6
I32	175.9 $\pm 0.4$	57.2 $\pm 0.6$	42.2 $\pm 0.6$	26.4 $\pm$ 0.5, 16.9 $\pm$ 0.6	13.7 $\pm 0.6$		124.7 $\pm 0.8$	-127.3 $\pm$ 7.0, 136.5 $\pm$ 7.9
G33	172.0 $\pm 0.5$	48.8 $\pm 0.5$					114.7 $\pm 0.8$	
L34	173.6 $\pm 1.7$	53.1 $\pm 0.8$	45.6 $\pm 0.7$	27.5 $\pm 0.7$	25.0 $\pm 0.5$		114.8 $\pm 1.0$	-130.1 $\pm$ 14.5, 141.2 $\pm$ 12.5
M35	173.6 $\pm 0.8$	53.8 $\pm 0.7$	36.9 $\pm 0.8$	31.8 $\pm 1.0$			121.6 $\pm 1.0$	-120.8 $\pm$ 11.1, 129.3 $\pm$ 5.9
V36	173.5 $\pm 0.8$	59.0 $\pm 0.7$	35.9 $\pm 0.6$	20.4 $\pm 1.0$			123.6 $\pm 1.1$	-132.9 $\pm$ 11.9, 142.9 $\pm$ 12.0
G37	171.2 $\pm 1.5$	46.5 $\pm 1.0$					111.6 $\pm 1.3$	-173.3 $\pm$ 13.9, -179.6 $\pm$ 13.9
G38	171.1 $\pm 1.0$	45.6 $\pm 1.0$					103.5 $\pm 2.5$	-173.2 $\pm$ 17.8, -179.3 $\pm$ 13.6
V39	173.6 $\pm 1.4$	60.4 $\pm 1.2$	34.3 $\pm 1.4$	20.7 $\pm 1.8$			118.6 $\pm 2.5$	-115.5 $\pm$ 17.7, 135.7 $\pm$ 9.3